DFT-UX3LYP Studies on the Coordination Chemistry of Ni^{2+}. Part 1: Six Coordinate $[Ni(NH_3)_n(H_2O)_{6-n}]^{2+}$ Complexes

Pradeep R. Varadwaj,[†,‡] Ignacy Cukrowski,*[,†] and Helder M. Marques*[,§]

Department of Chemistry, Natural and Agricultural Sciences 1, University of Pretoria, Pretoria, 0002 South Africa, Saha Institute of Nuclear Physics, Kolkata 700 064, West Bengal, India, and Molecular Sciences Institute, School of Chemistry, University of the Witwatersrand, Johannesburg, 2050 South Africa

Received: May 6, 2008; Revised Manuscript Received: July 28, 2008

DFT calculations with the UX3LYP hybrid functional and a medium-sized 6-311++G(d,p) basis set were performed to examine the gas-phase structure of paramagnetic ($S = 1$) six-coordinate complexes $[Ni(NH_3)_n(H_2O)_{6-n}]^{2+}$, $0 \le n \le 6$. Significant interligand hydrogen bonding was found in $[Ni(H_2O)_6]^{2+}$, but this becomes much less significant as NH_3 replaces H_2O in the coordination sphere of the metal. Bond angles and bond lengths obtained from these calculations compare reasonably well with available crystallographic data. The mean calculated Ni−O bond length in $[Ni(H_2O)_6]^{2+}$ is 2.093 Å, which is 0.038 Å longer than the mean of the crystallographically observed values (2.056(22) Å, 108 structures) but within 2σ of the experimental values. The mean calculated Ni−N bond length in $[Ni(NH_3)_6]^{2+}$ is 2.205(3) Å, also longer (by 0.070 Å) than the crystallographically observed mean (2.135(18) Å, 7 structures). Valence bond angles are reproduced within 1°. The successive replacement of H_2O by NH_3 as ligands results in an increase in the stabilization energy by 7 ± 2 kcal mol^{-1} per additional NH_3 ligand. The experimentally observed increase in the lability of H_2O in Ni(II) as NH_3 replaces H_2O in the coordination sphere is explained by an increase in the Ni−OH_2 bond length. It was found from a natural population analysis that complexes with the highest stabilization energies are associated with the greatest extent of ligand-to-metal charge transfer, and the transferred electron density is largely accommodated in the metal 4s and 3d orbitals. An examination of the charge density ρ_{bcp} and the Laplacian of the charge density $\nabla^2\rho_{bcp}$ at the metal−ligand bond critical points (bcp) in the series show a linear correlation with the charge transferred to the metal. Values of $\nabla^2\rho_{bcp}$ are positive, indicative of a predominantly closed-shell interaction. The charge transferred to the metal increases as n, the number of NH_3 ligands in the complex, increases. This lowers the polarizing ability of the metal on the ligand donors and the average metal−ligand bond length increases, resulting in a direct correlation between the dissociation energy of the complexes and the reciprocal of the average metal−ligand bond length. There is a strong correlation between the charge transferred to the metal and experimental ΔH values for successive replacement of H_2O by NH_3, but a correlation with stability constants ($\log \beta$ values) breaks when $n = 5$ and 6, probably because of entropic effects in solution. Nevertheless, DFT calculations may be a useful way of estimating the stability constants of metal−ligand systems.

1. Introduction

Nickel has a rich coordination chemistry and an exceptionally extensive organometallic chemistry[1] and plays an important role in biology.[2,3] Oxidation states ranging from −1 to +4 are known, but the +2 state is by far the most common. In its complexes the d^8 Ni^{2+} ion is usually 4-, 5-, or 6-coordinate and exhibits a range of coordination geometries that includes paramagnetic tetrahedral and octahedral complexes and diamagnetic square planar complexes.

Quantum mechanical calculations both at the SCF-HF, MP2, and DFT levels of theory have been performed on aqua complexes in the gas phase; these include studies on $[M(H_2O)_6]^{3+}$ ($M = Sc^{3+}$ to Fe^{3+}),[4] $[Mn(H_2O)_6]^{2+}$,[5] the hexaaqua Fe^{2+} and Fe^{3+} ions,[6] and the aqua complexes of Co^{2+},[7,8] Ni^{2+},[7−9] Cu^{2+},[7,10−12] and Zn^{2+}.[8,9,13−16] In a study of $[Ni(H_2O)_5L]^{2+}$ complexes ($L = H_2O$, CH_3OH, CH_3SCH, and NH_3) at the B3LYP level of theory in conjunction with a variety of basis sets ranging from 3-21G(d) to 6-311++G(d,p), Rulíšek and Havlas[9] have demonstrated that the B3LYP functional in conjunction with a 6-311+G(d,p) basis set is a computationally efficient method for the precise determination of molecular geometries and that reaction energies compared excellently with those obtained from high-level ab initio methods. Deeth and coworkers[17] conducted a comprehensive study on the ability of DFT methods to reproduce the observed crystallographic bond lengths of compounds of the type $[MA_nB_{m-n}]$ (M = Co(III), Ni(II), Pt(II); A and B a variety of N-, O-, P-, and C-donor ligands, Cl^-, CO) and showed that gas-phase calculations systematically overestimate the metal−ligand bond length and that effects such as the trans influence are not correctly reproduced; incorporation of environmental effects by explicitly including a solvation model significantly improves the agreement between the observed and the computed structures.

A few reports have appeared on the use of DFT methods to study mixed ammine-aqua complexes of the metal ions of the first-row d-block metals in the gas phase. It has been demonstrated that 4-coordinate mixed aqua-ammonia complexes of

* Corresponding authors. E-mail: Ignacy.Cukrowski@up.ac.za and Helder.Marques@wits.ac.za.
† University of Pretoria.
‡ Saha Institute of Nuclear Physics.
§ University of the Witwatersrand.

10.1021/jp803961s CCC: $40.75
Published on Web 09/30/2008

Cu^{2+} are energetically more stable than 5- and 6-coordinate complexes[11] and that it is energetically more favorable to have NH_3 rather than H_2O in the first coordination sphere of the metal. A similar conclusion was reached in a study on Zn^{2+}.[18]

Addition of NH_3 to an aqueous solution of the green octahedral hexahydrate cation $[Ni(H_2O)_6]^{2+}$ will result in the formation of a range of blue complexes of the type $[Ni(H_2O)_{6-n}(NH_3)_n]^{2+}$, reaching $n = 6$ when the $[NH_3]:[Ni^{2+}]$ ratio is $>10^3$. A search of the Cambridge Structural Database (CSD) and the Inorganic Crystal Structure Database (ICSD) gave seven reported structures for the $[Ni(NH_3)_6]^{2+}$ cation but only one structure, that of an unusual mixed salt, (triamminetriaquanickel(II)-diamminetetraaquanickel(II)-amminepentaaquanickel(II))bis(4-fluoro-3-sulfobenzylphosphonate) tetrahydrate,[19] for 6-coordinate Ni^{2+} with mixed H_2O and NH_3 ligands. There are over one hundred reported structures containing the $[Ni(H_2O)_6]^{2+}$ cation. There are no structures of Ni^{2+} containing more than six aqua ligands, as expected, given the energetic preference for the coordination of Ni^{2+} with six H_2O ligands over seven or eight ligands.[20]

No systematic theoretical study of the coordination of Ni^{2+} with mixed ammine-aqua ligands appears to have been reported. The bonding in these complexes is expected to be dominated by ion−dipole electrostatic interactions (although contributions arising from polarization, charge transfer, dispersion interactions, and exchange repulsive interactions at the equilibrium configuration of the complex are likely to be present). Because N has a lower electronegativity than O and is more polarizable, NH_3 forms the stronger bonds to metal ions. Because of this, the $Ni^{2+}-OH_2$ stretching frequency occurs at 405 cm^{-1} in the hexaaqua complex,[21] but the $Ni^{2+}-NH_3$ stretch is found at 435 cm^{-1} in $[Ni(NH_3)_4Cl_2]$.[22]

Despite its widespread use in examining the structure and energetics of transition-metal complexes, the B3LYP hybrid functional[23] is recognized to poorly estimate the interaction energy of weakly bound systems because of the lack of strong electron−electron correlation, although Werner-type complexes with relatively weak field ligands are usually accurately described with hybrid functionals.[24] It has been suggested[14] that this is the reason why this functional favors 4-coordinate $[Zn(H_2O)_4]^{2+}$ over 6-coordinate $[Zn(H_2O)_6]^{2+}$, whereas the Zn−O bond energy is underestimated.[15] B3LYP has more recently been extended by Goddard and co-workers to X3LYP (a generalized gradient approximation (GGA)-type hybrid functional in which X3 is an admixture of the extended Becke's three-parameter scheme[25] and a linear combination of the Becke's B88[26] and Perdew−Wang's PW91[27] exchange functionals and the LYP correlation[23]). This has been demonstrated to improve the description of softer interactions (van der Waals interactions, hydrogen bonding) while usually (but not always[28]) improving the predicted thermochemical values.[29−31]

In this paper, we report a computational study at the DFT-UX3LYP/6-311++G(d,p) level of theory of the structural, energetic and electronic properties of $S = 1$ Ni^{2+} complexes in the gas phase in their ground electronic states in the presence of n NH_3 ligands and $(6 - n)$ H_2O ligands ($n = 0-6$). We compare key computed structural metrics with crystallographic data to assess how well molecular geometry is predicted. We have investigated how the UX3LYP functional predicts trends in the energetics of nine different complexes of the type $[Ni(NH_3)_n(H_2O)_{6-n}]^{2+}$. For comparison purposes, we have also carried out single-point energy calculations at the UB3LYP level of theory on the UX3LYP-optimized geometry of these complexes. We have examined the effect of charge transfer onto the metal and the orbital occupancy of the metal on complex formation by using natural population bond orbital analysis and its relationship with the stabilization energies and metal−ligand bond lengths in the series. We have also examined the topological properties of electron charge densities and the Laplacian of the charge density at the Ni−N and Ni−O bond critical points (bcp) in order to gain insight into the nature of the bonding in these complexes. Finally, we explored trends between experimentally determined reaction enthalpies and overall complex formation constants with the parameters derived from this theoretical study. We are currently investigating the effect of solvent on the computed structures and also what occurs when we specify $S = 0$ in these systems; we will report our results elsewhere.

2. Computational Details

All calculations were carried out by using the GAUSSIAN 03 suite of programs.[32] Visualization of the structures and normal modes of harmonic vibration frequencies of these complexes were performed with the aid of GAUSSVIEW 03.[33]

The ligands (H_2O, NH_3) and complexes were optimized, respectively, at the restricted and unrestricted X3LYP levels of theory by computing the analytical first derivative of the relevant X3LYP potential-energy surfaces with respect to the atom-fixed nuclear coordinates. The ligands were symmetrized under C_{2V} (for H_2O) and C_{3V} (for NH_3) point groups. The complexes were constructed by placing the ligands in pseudo-octahedral, but random, orientation about the metal under the C_1 point group because we did not wish to presuppose any particular symmetry.

We performed frequency calculations by determining analytically the second derivatives of the UX3LYP potential energy surfaces with respect to the fixed nuclear coordinates to determine whether each of the minimized structures corresponded to an energy minimum or a saddle point. A tight gradient convergence criterion (necessary for analyzing the small structural variations in these complexes) with ultrafine integration grid was used in all calculations. On several occasions, while performing these calculations, we encountered SCF failures that caused termination of the calculations and in some cases produced structures with several imaginary frequencies. This is not unexpected because transition-metal complexes can lead to SCF convergence problems because of near-degenerate energies at the Fermi level. Where structures produced imaginary frequencies, ligands were rotated slightly along the donor-metal axis and reminimized. Several attempts would eventually lead to positive Hessian energy eigenvalues. All reported geometries belong to genuine minimum energy conformations.

For H_2O and NH_3 we assumed a singlet electronic ground state, whereas for $[Ni(NH_3)_n(H_2O)_{6-n}]^{2+}$ ($n = 0-6$), we used an unrestricted spin triplet-state formalism. A medium-sized basis set of valence triple Gaussian quality 6-311++G(d,p) augmented with both diffuse and polarization functions was used in the computation because this has been shown to give good estimates of geometric parameters and of energies comparable to those obtained from high-order ab initio methods.[9] The additional diffuse function helps with a more reliable description of the coordination environment around the metal ion and in estimating binding energies; the addition of a polarization function improves the prediction of bond angles. No relativistic effects were taken into account because these are considered unimportant for the first-row d-block metals.[9]

Atom-centered partial charges describe chemical systems in a well-behaved manner.[34] We therefore carried out natural population analysis[35−40] to determine the atom-centered partial charges on the minimum energy configuration of each complex

TABLE 1: Calculated (RX3LYP/6-311++G(d,p)) and Experimentally Observed Properties of the Ligands NH_3 and H_2O

		ZPVE/kcal mol^{-1}		dipole moment μ/D				structural metric/Å, deg			normal vibrational modes/cm^{-1}		
species	E/au[a]	Calc	Obs	Calc	Obs	ref		Calc	Obs	ref	Calc	Obs	ref
NH_3	−56.553915	21.53	20.63	1.69	1.47	64	N−H	1.014	1.039	65	3616 (E) 3486 (A_1) 1670 (E) 1005 (A_1)	3444 3337 1627 950	66
							H−N−H	107.96	106.7	65			
H_2O	−76.428823	13.38	12.88	2.16	1.85	67	O−H	0.962	0.957	68	3932 (B_2) 3827 (A_1) 1603 (A_1)	3756 3657 1595	66
							H−O−H	105.13	104.5	68			

[a] 1 au of E = 627.5095 kcal mol^{-1}.

by using the same level of theory in conjunction with a 6-311++G(d,p) 6D basis set. Additional diffuse functions were used to obtain a more refined description of the charge distribution in the compounds because it is recognized that the addition of such functions is required for an adequate description of charged systems.[41]

The transfer of electron density between the metal and the ligands as well as between the ligands themselves consequent on the loss of electron density from the natural localized bond orbitals of an idealized Lewis structure into empty non-Lewis orbitals was assessed in these complexes by computing the second-order stabilization energies between various donor−acceptor pairs of orbitals by natural localized molecular orbitals analysis by using the Natural Bond Orbitals NBO set of programs.[40] The wave functions were analyzed with the help of NBO by using the SCF density.[40] Equation 1 gives the second-order perturbative estimates of these stabilization energies $E^{(2)}$ associated with the delocalization $i \rightarrow j$ where q_i is the donor orbital occupancy, $F(i,j)$ is the off-diagonal NBO Fock matrix element, ε_i and ε_j are the diagonal elements representing the orbital energies, and i,j represents donor NBO(i) and acceptor NBO(j), respectively.[35−39,42]

$$E^{(2)} = \Delta E_{ij} = q_i F(i,j)^2/(\varepsilon_i - \varepsilon_j) \quad (1)$$

We carried out topological analysis of the electron charge density ($\rho(r)$) and the Laplacian of the charge density ($\nabla^2\rho(r)$) at the bcp's at the UX3LYP/6-311++G(d,p) 6D level by using the atoms in molecules framework of Bader.[43]

The overall binding energy E_b, without zero-point vibration corrections, and the dissociation energy, E_d^c, incorporating a zero-point vibrational correction, between the metal ion and the ligands (NH_3 and H_2O) were calculated by using eqs 2 and 3, respectively, where $n = 0-6$, ZPVE is the zero-point vibrational energy, and the E terms are the gas-phase total energies at 0 K.

$$E_b([Ni(NH_3)_n(H_2O)_{6-n}]^{2+}) = E([Ni(NH_3)_n(H_2O)_{6-n}]^{2+} - (E(Ni^{2+}) + nE(NH_3) + (6-n)E(H_2O)) \quad (2)$$

$$E_d^c([Ni(NH_3)_n(H_2O)_{6-n}]^{2+} = -E_b([Ni(NH_3)_n(H_2O)_{6-n}]^{2+} - \mathrm{ZPVE}([Ni(NH_3)_n(NH_2O)_{6-n}]^{2+} + (E(Ni^{2+}) + n\mathrm{ZPVE}(NH_3) + (6-n)\mathrm{ZPVE}(H_2O) \quad (3)$$

For comparison, we have also carried out single-point energy calculations at the UB3LYP/6-311++G(d,p) level of theory on the resulting UX3LYP/6-311++G(d,p) optimized geometries of the complexes.

3. Results and Discussion

Ligands. Values of the total molecular energies (E), zero-point vibrational energies (ZPVE), dipole moments (μ), and molecular geometry of NH_3 and H_2O, as predicted at the RX3LYP/6-311++G(d,p) level of theory, are summarized in Table 1. The N−H bond length is underestimated by 0.025 Å, but the O−H bond length is well reproduced. Bond angles are predicted to approximately 1° of the experimental values. The dipole moments are overestimated by 0.2−0.3 D as expected from DFT-SCF density calculations. The computed normal-mode harmonic vibrations match reasonably well with the corresponding experimental values. The discrepancy between the two is attributed mainly to the neglect of anharmonic force-field and medium effects and the use of a finite-size basis set.[44] The scaling factors 0.945−0.995 obtained from the ratio of experimental to the computed frequencies are typical for DFT methods.[45−48]

Structure and Energetics. The structures of the Ni(II) complexes investigated were determined by specifying an $S = 1$ electronic ground state. The uncorrected binding energies (E_b, eq 2), the dissociation energies (E_d^c, eq 3), the partial charge on the metal ion (Ni^Q), the charge transfer from the ligands to metal (ΔQ), the charge density (ρ_{bcp}), and the Laplacian of the charge density ($\nabla^2\rho_{bcp}$) at the metal−ligand bcp of the complexes for $[Ni(NH_3)_n(H_2O)_{6-n}]^{2+}$ ($n = 0-6$) obtained at the UX3LYP level of theory are summarized in Table 2. The corresponding uncorrected binding energies (E_b^{UB3LYP}) obtained from single-point calculations at the UB3LYP level of theory on the UX3LYP minimum energy geometries are also given for comparison.

Of all complexes studied, $[Ni(H_2O)_6]^{2+}$ is predicted to be the least stable, and the successive replacement of H_2O by NH_3 results in a monotonic increase in the stabilization of the complexes by 7 ± 2 kcal mol^{-1}, presumably because of the higher polarizability of NH_3. Our results are in agreement with a similar study on Cu^{2+} where it was reported that gas-phase $[Cu(H_2O)_6]^{2+}$ is less stable than $[Cu(NH_3)_6]^{2+}$ by 62 kcal mol^{-1}.[11] The uncorrected binding energies obtained at the UB3LYP level of theory show a trend similar to that of the UX3LYP values (Table 2), although the values are on average 4 kcal mol^{-1} lower. This is probably attributable to the inability of the UB3LYP to adequately describe weak interactions such as dispersion.

Ignoring the H atoms, the predicted structure of $[Ni(H_2O)_6]^{2+}$ is that of a distorted octahedron. The deviation from octahedral geometry is a consequence of the interaction between the H atom of one ligand and the O atom of a neighboring ligand (Figure 1). The six such interactions have an O···H distance of 2.67 Å and (O···H−O) angles between 88.97 and 89.19°. The O−Ni−O angle that encompasses the two interacting ligands is 85.1°, whereas the O−Ni−O angle where the interaction is absent is larger, 95.7° (Figure 1). A more detailed discussion of these weak interactions, and a brief supporting discussion on natural population and bond orbital analysis, is given in the Supporting Information.

The mean Ni−O bond length is 2.093 Å. A study of the structure of $[Ni(H_2O)_6]^{2+}$ performed by using B3LYP/6-311++G(d,p)[9] gave slightly shorter values, 2.087 Å, for the

TABLE 2: Stability and Electronic Properties of Aqua-, Ammine-, and Mixed-Ligand of $S = 1$ Complexes of Ni^{2+} as Determined at the UX3LYP Level of Theory[a]

complex	E_b/kcal mol^{-1}	E_d^c/kcal mol^{-1}	relative E_d^c/kcal mol^{-1}	E_b^{UBLYP}/ kcal mol^{-1}	Ni^Q/e	charge transfer, ΔQ/e	ρ_{bcp} (Ni−O)/ au	ρ_{bcp} (Ni−N)/ au	$\nabla^2\rho$ (Ni−O)$_{bcp}$/ au	$\nabla^2\rho$ (Ni−N)$_{bcp}$/ au	ΔH^{62}/ kcal mol^{-1}	log β^{62}
$[Ni(H_2O)_6]^{2+}$	−363.6	349.1	0.0	−359.1	1.498	0.502	0.0557(1)		0.3257(4)			
$[Ni(NH_3)(H_2O)_5]^{2+}$	−375.5	361.1	12.0	−371.1	1.461	0.539	0.0521(5)	0.0732	0.3052(22)	0.3133	−3.6	2.72
trans-$[Ni(NH_3)_2(H_2O)_4]^{2+}$	−382.0	367.7	18.6	−377.9	1.421	0.579	0.0465(12)	0.0711	0.2623(89)	0.3041	−7.3	4.88
cis-$[Ni(NH_3)_2(H_2O)_4]^{2+}$	−383.8	369.0	19.9	−379.6	1.412	0.588	0.0480(7)	0.0728(48)	0.2719(60)	0.2996(29)		
mer-$[Ni(NH3)_3(H_2O)_3]^{2+}$	−390.4	375.5	26.4	−386.3	1.373	0.627	0.0421(13)	0.0664(16)	0.2305(14)	0.2811 (19)	−11.0	6.54
fac-$[Ni(NH3)_3(H_2O)_3]^{2+}$	−392.0	376.6	27.5	−387.9	1.365	0.635	0.0433	0.0671	0.2336(1)	0.2872(1)		
trans-$[Ni(NH_3)_4(H_2O)_2]^{2+}$	−397.1	381.5	32.4	−393.2	1.337	0.663	0.0394	0.0619	0.2150	0.2630	−15.3	7.67
cis-$[Ni(NH_3)_4(H_2O)_4]^{2+}$	−397.8	382.4	33.3	−393.9	1.331	0.669	0.0387	0.0633(8)	0.2024	0.2703(35)		
$[Ni(NH_3)_5(H_2O)]^{2+}$	−403.4	387.6	38.5	−399.6	1.297	0.703	0.0314	0.0589(16)	0.1527	0.2502(90)	−18.4	8.33
$[Ni(NH_3)_6]^{2+}$	−408.2	392.2	43.1	−404.4	1.263	0.737		0.0542(4)		0.2285(21)	−22.6	8.30

[a] The uncorrected stabilization energies (E_b^{UB3LYP}) obtained by single-point energy calculation at the UB3LYP level on the UX3LYP optimized geometries are included for comparison. E_b is the uncorrected binding energy (eq. 2). E_d^c is the corrected energy (eq 3). Ni^Q is the partial charge on Ni in the complexes, and ΔQ ($= 2 - Ni^Q$) is the ligand-to-metal charge transfer. The charge density (ρ_{bcp}) and the Laplacian of the charge density ($\nabla^2\rho(Ni-O)_{bcp}$) at the bcp are in au (1 au of $\rho = 6.7483$ e Å^{-3}, and 1 au of $\nabla^2\rho = 24.099$ e Å^{-5}). Experimental reaction enthalpies ΔH are presumed, where appropriate, to be for formation of a mixture of isomers. Overall stability constants, as log β, in aqueous solution at 25° C and $\mu = 0$.

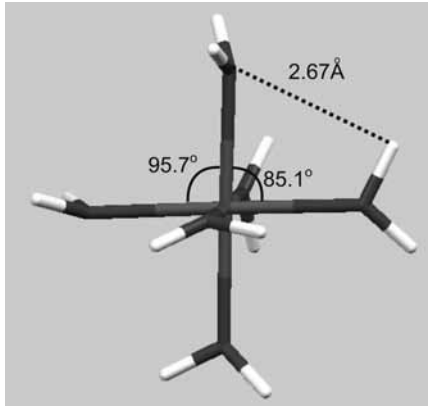

Figure 1. Predicted structure of $[Ni(H_2O)_6]^{2+}$ showing a nonbonded contact between an O atom of one ligand and an H on a neighboring ligand.

TABLE 3: Comparison of the Metrics of the Predicted UX3LYP/6-311++G(d,p) Level Structure of $[Ni(H_2O)_6]^{2+}$ and Structures Observed Crystallographically

		experimental[a]	
metric	predicted	mean (σ)	range
Ni−O /Å	2.0939(4)	2.056(22)	2.002–2.230
cis O−Ni−O /deg	90.0(5.2)	90.0(2.2)	80.0–99.3
trans O−Ni−O /deg	178.90(7)	179.2(1.8)	172.3–180.0
O−O−O face angle /deg	60.0(4.3)	60.0(1.7)	55.0–65.9

[a] From 108 structures in the CSD and ICSD.

Ni−O bonds, and in that study, there appears to be no indication of interligand nonbonded interactions of the type we observe here. This suggests that the X3LYP functional is able to describe nonbonded interactions better than the B3LYP functional. An average value of 2.108 Å for the Ni−O bond length has been reported at the HF-SCF level of theory elsewhere.[49]

There are 108 crystal structures in the CSD and ICSD that contain the $[Ni(H_2O)_6]^{2+}$ cation. As might be expected for condensed-phase data, there is considerable variation in the reported bond lengths and bond angles. Table 3 shows a comparison between our gas-phase structure of $[Ni(H_2O)_6]^{2+}$ and the crystallographic data. Deeth et al.[17] have reported that Co(III)−N bond lengths in a limited series of Co(III) hexaamine gas-phase structures calculated with B3LYP are overestimated by 0.05−0.08 Å compared to crystallographic structures, but the overestimation improves to 0.01−0.04 Å when the calculations incorporate a solvation model. We find that the Ni−O bond length is overestimated on average by 0.04 Å, and note that this is still within 1σ of the experimental mean of 108 solid-state structures. There is therefore no statistically significant difference between the values. It is clear that caution should be exercised when comparing calculated and experimental structures because of the often significant spread in the experimental values and a large body of experimental data is required before conclusions can be made. It appears that the level of theory used in this study, together with the chosen basis set, is appropriate for an accurate structural description of these systems.

Figure 2 shows the optimized six-coordinate complexes investigated in this study. On replacement of an H_2O ligand by NH_3 to form $[Ni(NH_3)(H_2O)_5]^{2+}$, the average Ni−O bond length increased from 2.093(0) to 2.113(2) Å. The van der Waals radius of N (1.55 Å) is larger than that of O (1.52 Å); this causes an increase in the steric repulsion between the ligands that is compensated for by their moving further apart (the average ligand−ligand distance increases by 0.021 Å). A consequence of this is that the O···H−O contacts diminish in importance and the O···H distance increases from on average 2.67 Å to between 2.78 and 2.99 Å. Consequently, Ni, O, and each of the latter's 2 H atoms are more nearly coplanar, and the interligand nonbonded interactions shown in Figure 1 have largely disappeared. Moreover, as a consequence of the better donor ability of NH_3 compared to that of H_2O, the net charge on the metal decreases from 1.498 e in $[Ni(H_2O)_6]^{2+}$ to 1.461 e in $[Ni(NH_3)(H_2O)_5]^{2+}$ (Table 1, and see Supporting Information). This decreases the polarizing ability of the metal, resulting in an overall increase in the average metal−ligand bond length.

The replacement of a second water molecule by another NH_3 ligand results in a further increase in the stability of the complex as noted above and in the average metal−ligand distance (Table 2). The trans isomer of $[Ni(NH_3)_2(H_2O)]^{2+}$ is 1.3 kcal mol^{-1} less stable than the cis isomer. In the trans isomer, all O−H bonds in a coordinated water molecule have the same length, indicating that none of the H atoms are involved in hydrogen bonding. On the other hand, NH protons interact weakly with lone pairs on O atoms with an average NH···O distance of 2.769(6) Å and an average N···O distance of 2.996(4) Å,

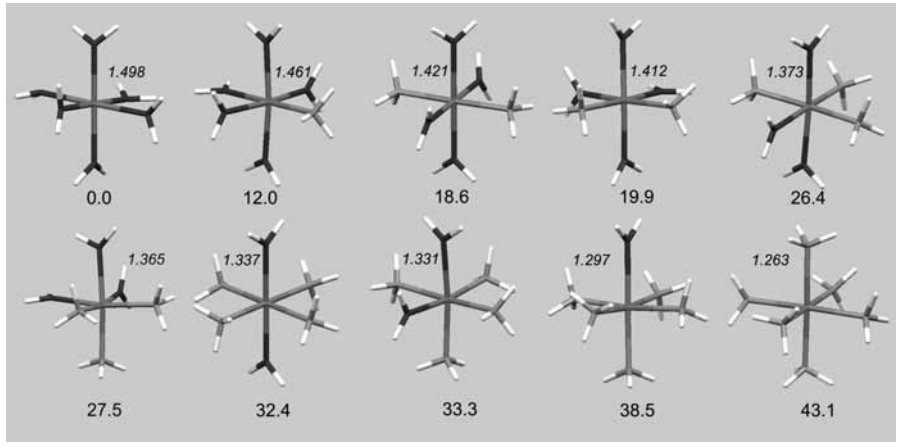

Figure 2. Structures of octahedral $[Ni(NH_3)_n(H_2O)_{6-n}]^{2+}$ predicted in this work. The molecular dissociation energies, E_d^c, relative to that of $[Ni(H_2O)_6]^{2+}$, are given (kcal mol^{-1}) below each structure. The partial charge (e) on the metal ion is given in italics above the metal.

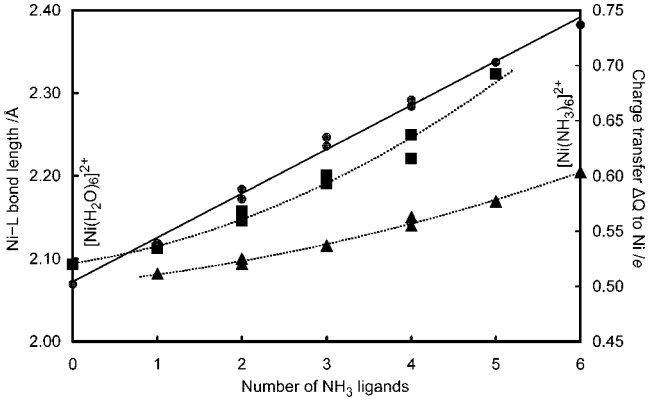

Figure 3. Dependence of the charge transfer, ΔQ (in e) onto Ni as a function of the number of NH_3 ligands, n, in $[Ni(NH_3)_n(H_2O)_{6-n}]^{2+}$ (●). The solid line is a linear regression line with $R^2 = 0.994$. Also shown are plots of the average Ni−O (■) and Ni−N (▲) bond lengths as a function n. The broken lines are merely to indicate trends. Multiple values for $n = 2$, 3, and 4 arise from isomers.

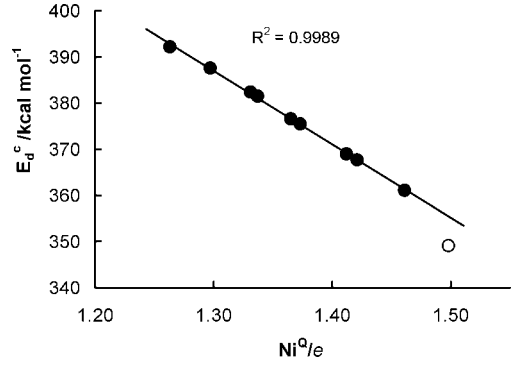

Figure 4. Correlation between the charge on Ni ion, Ni^Q, in complexes of the type $[Ni(NH_3)_n(H_2O)_{6-n}]^{2+}$ and the calculated dissociation energy of the complex. The point for $[Ni(H_2O)_6]^{2+}$ (○) has been excluded from the regression. (The inclusion of this point decreases R^2 to 0.976).

somewhat less than the sum of the van der Waals radii of O and N (3.07 Å). In the case of the cis isomer, the average NH···O contact is 2.81(12) Å, and the N···O distance is 2.89(6) Å. Thus, the average N···O distance in the trans isomer is about 0.1 Å longer than in the cis isomer, whereas the average interligand distances are about 0.043 and 0.028 Å longer, respectively, than in $[Ni(NH_3)(H_2O)_5]^{2+}$. We conclude that the ligand−ligand repulsion is less significant in the cis isomer than in the trans, resulting in a greater number of nonbonded weak interactions and a marginally more stable complex. Similar small differences in interligand interactions make *fac*-$[Ni(NH_3)_3(H_2O)_3]^{2+}$ marginally more stable (by 1.1 kcal mol^{-1}) than the mer isomer and *cis*-$[Ni(NH_3)_4(H_2O)_2]^{2+}$ more stable by 0.9 kcal mol^{-1} than the trans isomer.

The replacement of the second H_2O by NH_3 causes a further decrease in the partial charge on N (to 1.412 e in the cis isomer and 1.421 e in the trans isomer), a concomitant elongation of metal−ligand bonds, and an increase in ligand−ligand nonbonded distances. This trend continues as further H_2O molecules are replaced as ligands by NH_3. In Figure 3, we plot the charge transferred onto the metal, ΔQ, as a function of the number of NH_3 ligands in the complex. We also show how the average Ni−O and Ni−N bond lengths increase as the number of NH_3 ligands increases; the charge on the metal decreases, and its polarizing ability on the ligand electrons decreases. Because the bond energy is expected to vary inversely with bond length, there is, as expected, a direct correlation between the dissociation energy and the reciprocal of the average metal−ligand bond length (Figure S2 in the Supporting Information).

There is a virtually perfect linear correlation between the zero-point corrected dissociation energy and the charge on the Ni ion, Ni^Q, (Figure 4), provided that the value for $[Ni(H_2O)_6]^{2+}$ is excluded. The correlation indicates that this complex has a dissociation energy (by 6.3 kcal mol^{-1}) lower than expected, which suggests that the interligand hydrogen bonding in $[Ni(H_2O)_6]^{2+}$ noted above and largely absent in the rest of the complexes in this series impedes the effectiveness of the metal−ligand bonding and, at least in the gas phase, actually destabilizes the complex.

The rate constant for water exchange on $[Ni(H_2O)_6]^{2+}$ at 25 °C is 3.15×10^4 s^{-1} as measured by ^{17}O NMR methods;[50] this increases to 25×10^4 s^{-1} in $[Ni(NH_3)(H_2O)_5]^{2+}$, 61×10^4 s^{-1} in $[Ni(NH_3)_2(H_2O)_4]^{2+}$, and 250×10^4 M^{-1} in $[Ni(NH_3)_3(H_2O)_3]^{2+}$.[51,52] Our observation that the Ni−O bond length increases, and hence the bond weakens, as the number of NH_3 ligands increases provides an explanation for the increasing lability observed experimentally. Because the rate constants appear to increase exponentially with Ni−O bond length, we can estimate that the lifetime of $[Ni(NH_3)_4(H_2O)_2]^{2+}$ will be of the order of 0.5 ms and that of $[Ni(NH_3)_5(H_2O)]^{2+}$, in which the Ni−O bond length of 2.32 Å is longer than those in any experimentally observed hexa-aqua and mixed aqua-ammine complexes (Table S3 in the Supporting Information), about 20 ns. It would be very difficult if not impossible to measure these exchange processes by NMR methods.

Analysis of the Charge Density and the Laplacian of the Charge Density at the Metal−Ligand bcp. We carried out an analysis of the topological properties of electron density ρ_{bcp} and $\nabla^2\rho_{bcp}$ for all metal−ligand bonds and the covalent bonds within the ligands at the bcp. We found that ρ_{bcp} is small and positive and $\nabla^2\rho_{bcp} > 0$ for the metal−ligand bonds, whereas ρ_{bcp} is larger and $\nabla^2\rho_{bcp} < 0$ for the O−H or N−H covalent bonds. This is characteristic of interactions between closed-shell moieties and a covalent interaction, respectively. For example, in a study on the bcp properties of the electron density distribution in M−S bonds, $\nabla^2\rho_{bcp} > 0$ when M = Li, Na, Mg, and Al, but $\nabla^2\rho_{bcp} > 0$ for M = B, C, N, and P.[53] The value of $\nabla^2\rho_{bcp}$ at the N−C bond in histidine is −1.42 au[54] but 0.32 at the W−C bcp in $(CO)_5W-CHOH$.[55]

The values of ρ_{bcp} of the metal−ligand bonds were found to be relatively small compared to those for the covalent bonds. For example, ρ_{bcp} for the intramolecular O−H bonds in the complexes are in the range 0.353 au (in $[Ni(H_2O)_6]^{2+}$) to 0.357 au (in $[Ni(NH_3)_5(H_2O)]^{2+}$); the equivalent values for the N−H bonds hardly vary (0.331 au in $[Ni(NH_3)(H_2O)_5]^{2+}$ to 0.332 au for $[Ni(NH_3)_6]^{2+}$). The corresponding values of $\nabla^2\rho_{bcp}$ range from −0.254 to −0.252 au at the O−H bcps and from −0.157 to −0.154 au at the N−H bond bcps.

As NH_3 replaces H_2O in the complexes, ρ_{bcp}(Ni−O) decreases from 0.0557 au in $[Ni(H_2O)_6]^{2+}$ to 0.0314 au in $[Ni(H_2O)(NH_3)_5]^{2+}$, whereas ρ_{bcp}(Ni−N) decreases from 0.0732 au in $[Ni(NH_3)(H_2O)_5]^{2+}$ to 0.0542 au in $[Ni(NH_3)_6]^{2+}$ (Table 2). This accords with the calculated increase in the length of the metal−ligand bonds in this series of complexes.

The $\nabla^2\rho_{bcp}$ values for Ni−O and Ni−N bonds are positive and become less positive as the number of NH_3 ligands in these 6-coordinate complexes increases. The positive values of $\nabla^2\rho_{bcp}$ for metal−ligand bonds suggest that the bonds are predominantly ionic in character. There is a direct correlation between the partial charge on Ni and ρ_{bcp} (Figure S1A in the Supporting Information) and between the partial charge on Ni and $\nabla^2\rho_{bcp}$ (Figure S1B in the Supporting Information).

We interpret these observations as an increase in the covalent character of the metal−ligand bonding (ρ_{bcp} decreases, $\nabla^2\rho_{bcp}$ becomes less positive, and more charge is transferred to the metal) and a diffusion of charge density away from the bcps along the metal−ligand σ axis as O donors are replaced by less electronegative and more polarizable N donors.

Comparison with Experimental Stability Constants. There are significant differences between real solution equilibria and the theoretical modeling of transition-metal complexes such as that performed in this work. The limitations on computational resources at any reasonable level of theory usually limits studies of transition metal complexes to a gas-phase system consisting of the metal ion, the ligands needed to saturate the inner coordination sphere, and perhaps, enough ligands or solvent molecules to saturate the outer coordination sphere.[56] In the present study, our system was limited to Ni^{2+} and the six ligands required to form the $S = 1$ octahedral complexes of the metal. Thus, a system comprising Ni^{2+} and six NH_3 molecules produced the hexa-ammine complex. In reality, a very large excess of ammonia is required to be present in aqueous solution to form this species as is demonstrated in Figure S3 in the Supporting Information. Even with a 10-fold excess of ammonia (Figure S3a in the Supporting Information), one would be able to experimentally establish the stability constant only of the ML complex by employing glass-electrode potentiometry, the most commonly used experimental technique in the field. (For convenience, by M we mean the hexaaqua ion and by ML_n we mean $[Ni(NH_3)_n(H_2O)_{6-n}]$ and charges are omitted.) The precipitation of $Ni(OH)_2(s)$ will occur prior to the formation of all the consecutive complexes with ammonia (ML_2 to ML_6) and all possible $Ni_x(OH)_y$ species (see Table S2 in the Supporting Information). These species are shown in Figure S3 in the Supporting Information only to indicate what kind of complexes would be present if precipitation somehow could be avoided. Even in the (theoretical) absence of precipitation, the stability constants of ML_4, ML_5, and ML_6 could not be established as these complexes are not formed to a measurable concentration level even under a 10-fold ligand excess and at the total metal-ion concentration of 1 mM (Figure S3a in the Supporting Information).

Second, in aqueous solution, the complex formation equilibria are pH-dependent, and this has several important implications. Below about pH 4.5, Ni^{2+} does not form complexes with ammonia at all, even with a 2000-fold excess of ammonia, and ML_6 only starts to form above pH of 8 (Figure S3c in the Supporting Information).

The third significant difference is that, in aqueous solution, there are competing equilibria, such as a protonation reaction in which a ligand might be involved. This means that, in principle, the complex formation reaction will also involve a protonated form of a ligand (here NH_4^+), so that the formation of a complex ML should be written as in eq 4.

$$[Ni(H_2O)_6]^{2+} + NH_4^+ \rightleftarrows [Ni(NH_3)(H_2O)_5]^{2+} + H_3O^+ \quad (4)$$

There is usually a very significant difference between any system that can be modeled by computational methods and the system from which experimental data can be obtained. It would therefore be surprising indeed if there was an exact correlation between computationally determined parameters and experimentally derived data; at best, all one can reasonably expect is a trend between the two sets. Moreover, as has been pointed out,[57] it is not immediately obvious whether it is appropriate to compare the results of zero-temperature gas-phase DFT calculations to the condensed-phase finite-temperature experimental data which are typically available for the compounds of interest.

Notwithstanding these caveats, of undoubted interest to a coordination chemist is whether DFT data such as those that we have reported here correlate with experimental data. Agreement between calculated and experimental values where the latter are available for gas-phase reactions can be quite good,[58,59] but gas-phase data are not often available.

Several groups have sought to correlate theoretical results with experimental data obtained in solution. Because of the effect of the condensed phase, numerical agreement may be poor, but trends may nevertheless be informative. For example, a linear correlation between the pK_a of $[M(H_2O)_6]^{3+}$ and ΔE_{H^+} determined by DFT methods, where ΔE_{H^+} is the ZPVE-corrected difference in binding energies between $[M(OH)(H_2O)_5]^{2+}$ and $[M(H_2O)_6]^{3+}$ for a series of trivalent metal ions, has been reported.[60] Hancock and Bartolotti[61] used DFT methods to predict ΔG_{DFT} for the reaction $[M(H_2O)_6]^{n+} + NH_3 \rightarrow [M(H_2O)_5NH_3]^{n+} + H_2O$ for 36 metal ions and compared the values with experimental ΔG values or ΔG values estimated from a variety of empirical correlations. Correlations with $R^2 > 0.97$ were found, prompting these workers to suggest that such approaches could be useful for estimating experimentally inaccessible stability constants.

In Table 2, we list the experimental overall formation constants, as log β, obtained from a standard compilation[62] and the corresponding ΔH values for the reactions (25 °C and ionic strength $\mu = 0$ (eq 5)).

$$[Ni(H_2O)_6]^{2+}(aq) + nNH_3(aq) \rightarrow [Ni(NH_3)_n(H_2O)_{6-n}]^{2+}(aq) + nH_2O \quad (5)$$

There is a strong correlation ($R^2 = 0.995$) between log β and ΔQ for the complexes $[Ni(NH_3)_n(H_2O)_{6-n}]^{2+}$ for $1 \le n \le 4$, but it breaks down for $n = 5$ and 6 (Figure 5A), for which the experimental log β values are smaller than expected. It is noteworthy that the experimentally reported log $\beta_6 = 8.30$ is virtually identical to log β_5 (= 8.33) at ionic strength $\mu = 0$. The correlation between ΔQ and the reaction enthalpies, ΔH_{exp}, for the reactions of eq 5 persists for all species (Figure 5B). It appears that deviations in Figure 5A are a consequence of entropic effects in solution, probably because of the high $[NH_3]$:$[Ni^{2+}]$ ratios needed to form ML_5 and ML_6 (see Figure S3 in the Supporting Information). These observations suggest for the first time that it should be possible to predict a change in ΔH from DFT-computed values of ΔQ and hence to decide on the relative importance of enthalpic and entropic contributions to the stability of a complex.

A further indication that deviations between the experimental data and our calculated values occur because of the experimental conditions needed to form species such as ML_5 and ML_6 is found when we define the relative dissociation energy, Relative(E_d^c), as $E_d^c(ML_n) - E_d^c(M)$ and then compare the values of Relative(E_d^c) and ΔH_{exp} (Figure 6). There is a good linear relationship between the two variables for the reactions $n =$ 1−5 (eq 5,) provided that data obtained at low ionic strength are used. Deviations from this regression increase with increasing ionic strength, and the value for $[Ni(NH_3)_6]^{2+}$ deviates somewhat.

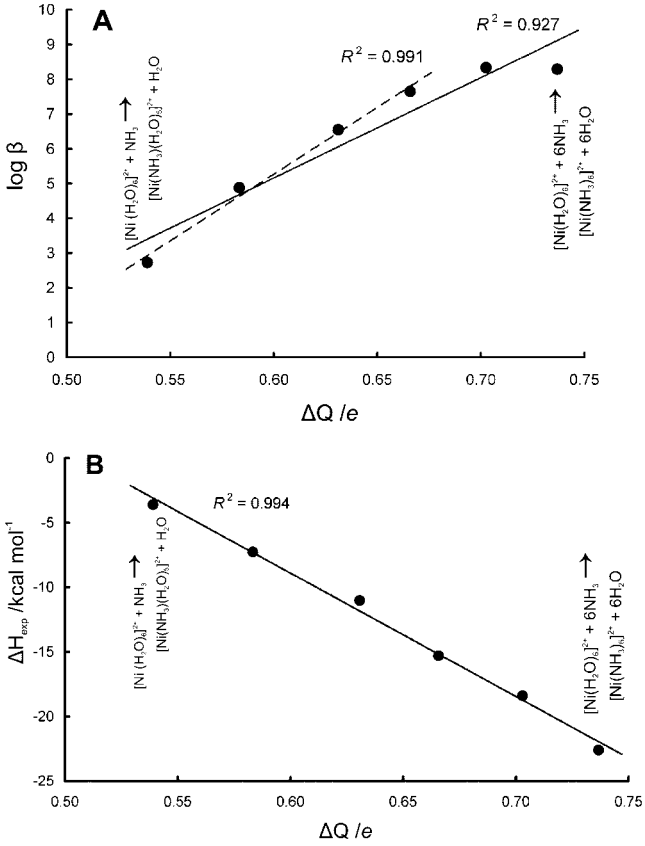

Figure 5. (A) Correlation between the charge transferred to the nickel ion in complexes of the type $[Ni(NH_3)_n(H_2O)_{6-n}]^{2+}$ and the experimentally observed log β values in aqueous solution. The good correlation observed between ΔQ and log β for $[Ni(NH_3)(H_2O)_5]^{2+}$, $[Ni(NH_3)_2(H_2O)_4]^{2+}$, $[Ni(NH_3)_3(H_2O)_3]^{2+}$, and $[Ni(NH_3)_4(H_2O)_2]^{2+}$ (dashed line) breaks down for $[Ni(NH_3)_5(H_2O)]^{2+}$ and $[Ni(NH_3)_6]^{2+}$. (B) There is a strong correlation between the experimental reaction enthalpy, ΔH_{exp}, and ΔQ for the formation of all $[Ni(NH_3)_n(H_2O)_{6-n}]^{2+}$ species.

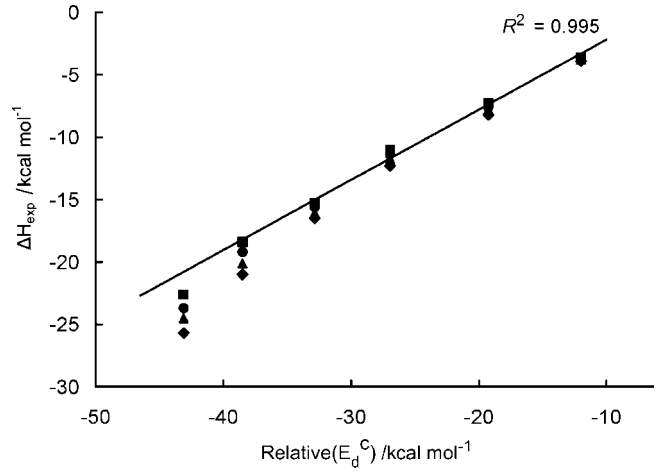

Figure 6. Correlation between the relative ΔE_d^c values (see text for definition) and experimental reaction enthalpies for the successive displacement of H_2O by NH_3 in six-coordinate Ni^{2+} complexes. Experimental data for $\mu = 0$ or 0.1 (■), 1 (●), 2 (▲), and 3 (◆) M. (The regression line is through data at $\mu = 0$ or 0.1 M and excludes the point for formation of $[Ni(NH_3)_6]^{2+}$. Inclusion of that point reduces R^2 to 0.990).

An analysis of the reported stability constants is shown in Table S3 in the Supporting Information. A small increase in the stability constants is observed with an increase in the ionic strength of the solution. At the same time, $\Delta\log\beta = (\log\beta_{n+1} - \log\beta_n)_\mu$ decreases as we proceed from ML to ML_6. An analysis of the reported experimental reaction enthalpies (ΔH, kcal mol^{-1}) of complex formation reaction between Ni^{2+} and NH_3 in aqueous solutions at 25 °C at the specified ionic strength is given in Table S4 in the Supporting Information. ΔH decreases monotonically, as expected, on going from ML to ML_6. Interestingly, the differences $\Delta(\Delta H_{MLn}) = (\Delta H_{MLn+1} - \Delta H_{MLn})_\mu$ remain quite constant at a particular ionic strength, and they do not vary significantly with ionic strength. For instance, the average value of $\Delta(\Delta H_{MLn})$ is -4.0 ± 0.4 and -4.1 ± 0.4 kcal mol^{-1} for $\mu = 1$ and 2 M, respectively. This rationalizes the linear correlations of Figures 5B and 6.

A similar analysis is given in Table S5 in the Supporting Information for the reported experimental reaction entropies (ΔS, cal K^{-1} mol^{-1}). In this case, we note that $\Delta(\Delta S_{MLn})_\mu$ increases significantly with n, confirming our conclusion that the cause of the deviation in Figure 5A is entropic in origin.

We now turn our attention to the change in dissociation energies ΔE_d^c (see Table 2) on successive replacement of H_2O by NH_3 on Ni^{2+} and examine whether there is a significant correlation between this quantity and changes in the reported stability constants at different ionic strengths. By assuming that all possible isomers of complexes examined here exist at comparable concentrations in a solution, we use an average value for E_d^c for the cis and trans and for the mer and fac isomers where appropriate (see Table S6 in the Supporting Information where differences in E_d^c are shown together with appropriate differences in stability constants at two ionic strengths). The variation in $\Delta E_d^c = (E_d^c(ML_{n+1}) - E_d^c(ML_n))_\mu$ versus $\Delta\log\beta = (\log\beta_{n+1} - \log\beta_n)_\mu$ for Ni^{2+} complexes with NH_3 in aqueous solutions at 25 °C at ionic strength $\mu = 0$ and 2 M is shown in Figure 7A.

There is a clear, but relatively weak, linear relationship between the quantities. When we assumed that the cis complexes

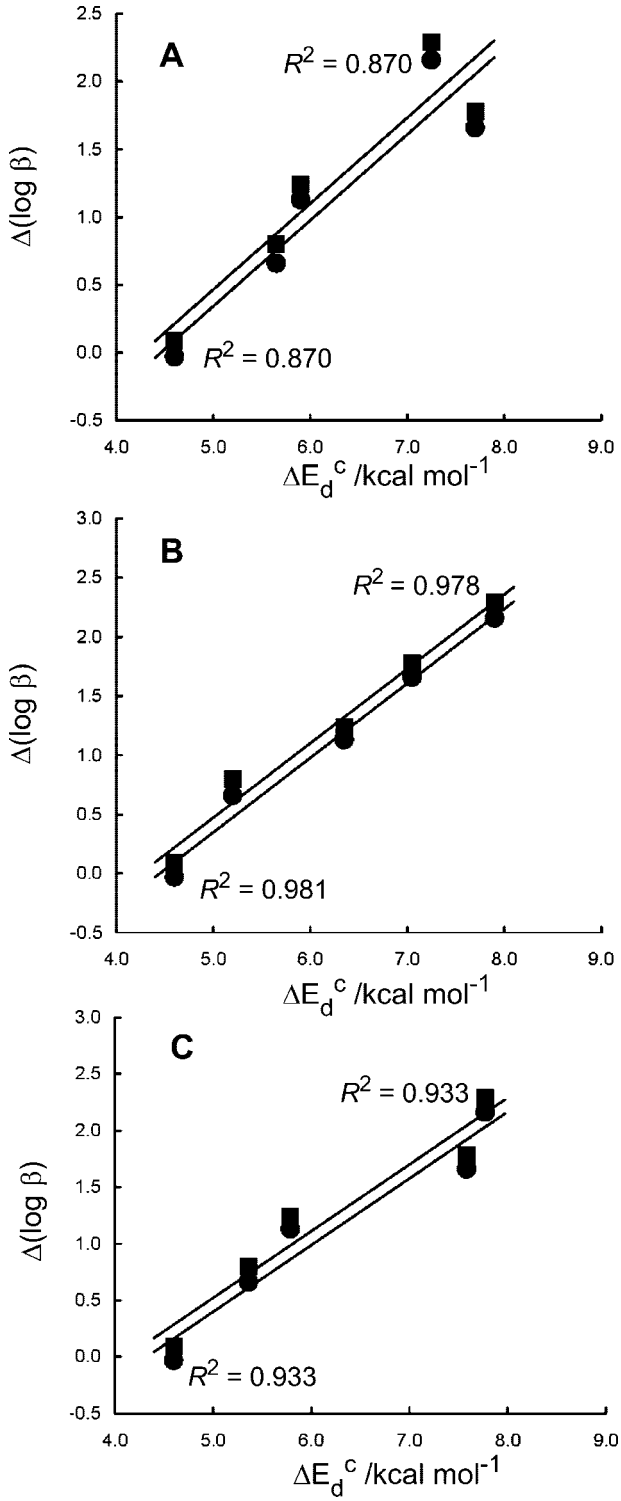

Figure 7. Variation in $\Delta E_d^c = (E_d^c(ML_{n+1}) - E_d^c(ML_n))_\mu$ versus $\Delta\log \beta = (\log \beta_{n+1} - \log \beta_n)_\mu$ for Ni^{2+} complexes with NH_3 in aqueous solutions at 25 °C at ionic strength $\mu = 0$ M (●) and 2 M (■). In panel **A**, we assume that cis and trans ML_2, mer and fac ML_3, and cis and trans ML_4 exist is equal proportions in solution. In panel **B**, we assume that ML_2 and ML_4 exist exclusively as the cis isomer in solution, but ML_3 is an equimolar mixture of the mer and fac isomers. To obtain the data in panel **C**, we used a population-weighted average of E_d^c for ML_2, ML_3, and ML_4 by determining the relative population of each by using a Boltzmann distribution.

of ML_2 and ML_4 exist as the predominant species in solution (they have marginally larger dissociation energies than trans isomers) but mer and fac isomers are both present in a solution (Table S6 in the Supporting Information), a significant improvement in linearity between ΔE_d^c and $\Delta\log \beta$ is observed (Figure 7B). By using the computed values of E_d^c, we determined the fraction population of each isomer of ML_2, ML_3, and ML_4 from a Boltzmann distribution and then calculated a population-weighted value for E_d^c for each species (this assumes, of course, that the difference in stability of the isomers that we calculated in the gas phase remains unaltered in aqueous solution). By using these values, we find (Figure 7C) a somewhat poorer correlation than that in Figure 7C. This suggests that, because of the effect of the environment, the relative energies in a condensed phase are somewhat different in the gas phase and that ML_2 and ML_4 exist in solution predominantly as the cis isomer, whereas both mer and fac isomers of ML_3 occur in solution.

If the relationship demonstrated in Figure 7 is applicable to other systems—and this validity of course still has to be demonstrated,—it offers interesting possibilities. First, it suggests that it may be possible to identify indirectly whether a species which could exist as one of two isomers in solution is indeed present as a mixture of geometrical isomers or whether either one or the other predominates. Second, it would provide a way of at least estimating stability constants from DFT methods. This is always of great interest in coordination chemistry because of difficulties that may arise in determining these quantities by experimental methods.[63]

4. Summary

The structures of all the complexes $[Ni(NH_3)_n(H_2O)_{6-n}]^{2+}$, $0 \le n \le 6$, were determined at the UX3LYP/6-311++G(d,p) level of theory. We found that there is significant interligand hydrogen bonding in $[Ni(H_2O)_6]^{2+}$ but that this becomes much less significant as NH_3 replaces H_2O in the coordination sphere of the metal. Bond angles and bond lengths obtained from these calculations compare well with crystallographic data, where available. The successive replacement of H_2O by NH_3 as ligands results in a monotonic increase in the average metal−ligand bond length and an increase in the stabilization energy of 7 ± 2 kcal mol^{-1} per additional NH_3 ligand. A similar trend has been found with UB3LYP level single-point energy calculations on the UX3LYP optimized geometry of these complexes. The UB3LYP values are about 4 kcal mol^{-1} lower in energy because the functional is inadequate for describing weak interactions such as dispersion. Correction for the zero-point vibrational energy at the UX3LYP level reduces the uncorrected binding energies of these complexes by about 4%.

We carried out a natural population analysis (Table 4) to estimate the extent of charge transfer between the ligands and the metal and orbital occupancy of the metal ion in these complexes. We found that complexes with the highest stabilization energies are associated with the greatest extent of ligand-to-metal charge transfer, which is largely accommodated in the metal 4s and 3d orbitals.

An examination of the electron density ρ_{bcp} and the Laplacian of the charge density $\nabla^2\rho_{bcp}$ at the metal−ligand bcp in the series show a linear correlation with Ni^Q, the charge on the metal. Both quantities are somewhat smaller at the Ni−O bcps than at the Ni−N bcps, reflecting the greater polarizability of N than that of O because of its lower electronegativity and the somewhat greater covalent character in the Ni−N than in the Ni−O bonds.

Several significant correlations were found. The charge transferred to the metal increases as n, the number of NH_3 ligands in the complex, increases. We suggest that this lowers

TABLE 4: Electron Population of Atomic 4s and 3d Valence Orbitals of Nickel Based on Natural Population Analysis Calculated at the UX3LYP/6-311++G(d,p) 6D Level of Theory[a]

		4s /e		3d /e						
complex	spin density	individual	total	*xy*	*xz*	*yz*	$x^2 - y^2$	z^2	$\alpha_{total}/\beta_{total}$	total
$[Ni(H_2O)_6]^{2+}$	α	0.130	0.263	0.997	0.997	0.997	0.996	0.997	4.984	8.205
	β	0.133		0.402	0.395	0.712	0.923	0.789	3.221	
$[Ni\ (NH_3)(H_2O)_5]^{2+}$	α	0.140	0.280	0.997	0.996	0.997	0.997	0.997	4.984	8.227
	β	0.140		0.988	0.993	0.175	0.331	0.756	3.243	
trans-$[Ni(NH_3)_2(H_2O)_4]^{2+}$	α	0.154	0.302	0.997	0.996	0.996	0.997	0.994	4.980	8.243
	β	0.148		0.997	0.995	0.995	0.090	0.186	3.263	
cis-$[Ni(NH_3)_2(H_2O)_4]^{2+}$	α	0.149	0.300	0.996	0.996	0.996	0.996	0.996	4.980	8.253
	β	0.151		0.723	0.357	0.897	0.590	0.706	3.273	
mer-$[Ni(NH3)_3(H_2O)_3]^{2+}$	α	0.161	0.319	0.997	0.996	0.996	0.997	0.994	4.980	8.273
	β	0.158		0.363	0.992	0.993	0.750	0.195	3.293	
fac-$[Ni(NH3)_3(H_2O)_3]^{2+}$	α	0.158	0.320	0.996	0.996	0.996	0.996	0.996	4.980	8.282
	β	0.162		0.448	0.438	0.702	0.922	0.792	3.302	
trans-$[Ni(NH_3)_4(H_2O)_2]^{2+}$	α	0.168	0.335	0.996	0.996	0.994	0.995	0.995	4.976	8.289
	β	0.167		0.996	0.996	0.218	0.330	0.773	3.313	
cis-$[Ni(NH_3)_4(H_2O)_2]^{2+}$	α	0.166	0.334	0.996	0.996	0.996	0.996	0.994	4.978	8.298
	β	0.168		0.493	0.995	0.992	0.646	0.194	3.320	
$[Ni(NH_3)_5(H_2O)]^{2+}$	α	0.173	0.348	0.996	0.996	0.995	0.995	0.995	4.977	8.316
	β	0.176		0.995	0.978	0.995	0.164	0.207	3.339	
$[Ni(NH_3)_6]^{2+}$	α	0.178	0.362	0.995	0.995	0.995	0.995	0.995	4.975	8.333
	β	0.184		0.479	0.630	0.486	0.920	0.843	3.358	

[a] The analysis of the individual electron occupancies are given separately for α and *β* spins.

the polarizing power of the metal on the ligands and causes the average metal−ligand bond length to increase. Consequently there is a direct relationship between the dissociation energy of the complexes and the reciprocal of the average metal−ligand bond length. There is a strong correlation between the charge transferred to the metal and experimental ΔH values for successive replacement of H_2O by NH_3, but a correlation with log *β* values breaks down for $n = 5$ and 6, which we attributed to entropic effects in solution. These results suggest that DFT calculations may be a useful way of estimating the stability constants of metal−ligand systems. It also appears from the results reported here that a combination of DTF calculations and solution chemistry might assist in predicting the predominant species present in solution when more than one isomer might be formed.

Acknowledgment. P.R.V. gratefully acknowledges the Director S.I.N.P. for leave to visit the University of Pretoria and gratefully thanks I.C. for the invitation, rewarding support, and funding. I.C. gratefully acknowledges financial support from National Research Foundation and the University of Pretoria. H.M.M gratefully acknowledges funding by the South African Research Chairs Initiative of the Department of Science and Technology administered by the National Research Foundation, the Mellon Foundation through grants administered by the University of the Witwatersrand, and the University Research Committee of the University of the Witwatersrand. We would like to thank Prof. Dr. Rudi van Eldik for useful discussions.

Supporting Information Available: This consists of a discussion on the weak interactions between H_2O ligands in $[Ni(H_2O)_6]^{2+}$, a note on the hydrogen bonding in $[Ni(H_2O)_6]^{2+}$, and a description of a natural population and bond-orbital analysis on the complexes investigated in this work. Figures show the dependence of the electron density and the Laplacian of the electron density for Ni−O and Ni−N bonds in $[Ni(NH_3)_n(H_2O)_{6-n}]^{2+}$ on the partial charge on the nickel ion, the dependence of the dissociation energy on the reciprocal of the average metal−ligand bond in $[Ni(NH_3)_n(H_2O)_{6-n}]^{2+}$, and simulated species distribution diagrams for the Ni(II)−NH_3 system. Tables give a comparison of selected structural metrics of the calculated structures and those observed crystallographically, values of equilibrium constants used to calculate the species distribution diagrams of the Ni-NH_3 system, an analysis of the reported overall stability constants, of the reported experimental reaction enthalpies, and of the experimental reaction entropies for the Ni−NH_3 system, and data used in Figure 7 of the text. This information is available free of charge via the Internet at http://pubs.acs.org.

References and Notes

(1) Cotton, F. A.; Wilkinson, G. *Advanced Inorganic Chemistry,* 5th ed.; John Wiley & Sons: New York, NY, 1988.
(2) Evans, D. J.; Pickett, C. J. *Chem. Soc. Rev.* **2003**, *32*, 268.
(3) Evans, D. J. *Coord. Chem. Rev.* **2005**, *249*, 1582.
(4) Kallies, B.; Meier, R. *Inorg. Chem.* **2001**, *40*, 3101.
(5) Trzaskowski, B.; Les, A.; Adamowicz, L. *Int. J. Mol. Sci.* **2003**, *4*, 503.
(6) Jarzêcki, A. A.; Anbar, A. D.; Spiro, T. G. *J. Phys. Chem. A* **2004**, *108*, 2726.
(7) Kai, E.; Nishimoto, K. *Int. J. Quantum Chem.* **1980**, *18*, 403.
(8) Rulíšek, L.; Havlas, Z. *J. Chem. Phys.* **2000**, *112*, 149.
(9) Rulíšek, L.; Havlas, Z. *J. Phys. Chem. A* **1999**, *103*, 1634.
(10) El-Nahas, A. M.; Tajima, N.; Hirao, K. *Chem. Phys. Lett.* **2000**, *318*, 333.
(11) Pavelka, M.; Burda, J. V. *Chem. Phys.* **2005**, *312*, 193.
(12) Bérces, A.; Nukada, T.; Margl, P.; Ziegler, T. *J. Phys. Chem. A* **1999**, *103*, 9693.
(13) Lee, S.; Kim, J.; Park, J. K.; Kim, K. S. *J. Phys. Chem.* **1996**, *100*, 14329.
(14) Díaz, N.; Suárez, D.; Merz, K. M. *Chem. Phys. Lett.* **2000**, *326*, 288.
(15) Smith, G. D.; Bell, R.; Borodin, O.; Jaffe, R. L. *J. Phys. Chem. A* **2001**, *105*, 6506.
(16) Pavlov, M.; Siegbahn, P. E. M.; Sandström, M. *J. Phys. Chem. A* **1998**, *102*, 219.
(17) Hocking, R. K.; Deeth, R. J.; Hambley, T. W. *Inorg. Chem.* **2007**, *46*, 8238.
(18) Kim, K. S.; Lee, S.; Mhin, B. J.; Cho, S. J.; Kim, J. *Chem. Phys. Lett.* **1993**, *216*, 309.
(19) Benedetto, A. F.; Squattrito, P. J.; Adam, T.; Montoneri, E. *Inorg. Chim. Acta* **1997**, *260*, 207.
(20) Rodriguez-Cruz, S. E.; Jockusch, R. A.; Williams, E. R. *J. Am. Chem. Soc.* **1998**, *120*, 5842.
(21) Nakagawa, I.; Shimanuchi, T. *Spectrocihim. Acta* **1964**, *20*, 430.
(22) Clark, R. J. H.; Williams, C. S. *J. Chem. Soc. A* **1966**, 1425.

(23) Stephens, P. J.; Devlin, J. F.; Chabalowski, C. F.; Frisch, M. J. *J. Phys. Chem.* **1994**, *98*, 11623.
(24) Harvey, J. N. *Annu. Rep. Prog. Chem., Section C* **2006**, *102*, 203.
(25) Becke, A. D. *J. Chem. Phys.* **1993**, *98*, 5648.
(26) Becke, A. D. *Phys. Rev. A* **1988**, *38*, 3098.
(27) Perdew, J. P. In *Electronic Structure of Solids*; Ziesche, P.; Eschrig, H., Eds.; Akademie Verlag: Berlin, 1991; pp 11.
(28) Černý, J.; Hobza, P. *Phys. Chem. Chem. Phys.* **2005**, *7*, 1624.
(29) Xu, X.; Goddard, W. A. *Proc. Natl. Acad. Sci. U.S.A.* **2004**, *101*, 2673.
(30) Xu, X.; Goddard, W. A. *J. Phys. Chem. A* **2004**, *108*, 2305.
(31) Xu, X.; Zhang, Q.; Muller, R. P.; Goddard, W. A. *J. Chem. Phys.* **2005**, *122*, 014105.
(32) Frisch, M. J.; Trucks, G. W.; Schlegel, H. B.; Scuseria, G. E.; Robb, M. A.; Cheeseman, J. R.; Montgomery, J. A., Jr.; Vreven, T.; Kudin, K. N.; Burant, J. C.; Millam, J. M.; Iyengar, S. S.; Tomasi, J.; Barone, V.; Mennucci, B.; Cossi, M.; Scalmani, G.; Rega, N.; Petersson, G. A.; Nakatsuji, H.; Hada, M.; Ehara, M.; Toyota, K.; Fukuda, R.; Hasegawa, J.; Ishida, M.; Nakajima, T.; Honda, Y.; Kitao, O.; Nakai, H.; Klene, M.; Li, X.; Knox, J. E.; Hratchian, H. P.; Cross, J. B.; Bakken, V.; Adamo, C.; Jaramillo, J.; Gomperts, R.; Stratmann, R. E.; Yazyev, O.; Austin, A. J.; Cammi, R.; Pomelli, C.; Ochterski, J. W.; Ayala, P. Y.; Morokuma, K.; Voth, G. A.; Salvador, P.; Dannenberg, J. J.; Zakrzewski, V. G.; Dapprich, S.; Daniels, A. D.; Strain, M. C.; Farkas, O.; Malick, D. K.; Rabuck, A. D.; Raghavachari, K.; Foresman, J. B.; Ortiz, J. V.; Cui, Q.; Baboul, A. G.; Clifford, S.; Cioslowski, J.; Stefanov, B. B.; Liu, G.; Liashenko, A.; Piskorz, P.; Komaromi, I.; Martin, R. L.; Fox, D. J.; Keith, T.; Al-Laham, M. A.; Peng, C. Y.; Nanayakkara, A.; Challacombe, M.; Gill, P. M. W.; Johnson, B.; Chen, W.; Wong, M. W.; Gonzalez, C.; Pople, J. A. *Gaussian 03*, Revision D.01; Gaussian, Inc.: Wallingford, CT, 2004.
(33) Dennington, R.; Keith, T.; Millam, J.; Eppinnett, K.; Hovell, W. L.; Gilliland, R. *GaussView; 3.09 ed.*; Semichem, Inc.: Shawnee Mission, 2003.
(34) Levy, J. B. *Structural Chem.* **1999**, *10*, 121.
(35) Foster, J. P.; Weinhold, F. *J. Am. Chem. Soc.* **1980**, *102*, 7211.
(36) Reed, A. E.; Weinhold, F. *J. Chem. Phys.* **1983**, *78*, 4066.
(37) Reed, A. E.; Weinhold, F. *J. Chem. Phys.* **1985**, *83*, 1736.
(38) Reed, A. R.; Weinstock, R. B.; Weinhold, F. *J. Chem. Phys.* **1985**, *83*, 735.
(39) Reed, A. E.; Curtiss, L. A.; Weinhold, F. *Chem. Rev.* **1988**, *88*, 899.
(40) Glendening, E. E.; Reed, A. E.; Carpenter, J. E.; Weinhold, F. *NBO (Natural Bond Orbital)*, v. 3.0, as implemented in GAUSSIAN 03, Gaussian Inc.: Wallingford, CT, 2004.
(41) Hehre, W. J.; Radom, L.; Schleyer, P. v. R. J. A.; Pople, J. A. *Ab Initio Molecular Orbital Theory*; Wiley: New York, 1986.
(42) Weinhold, F.; Landis, C. R. *Chem. Educ. Res. Pract. Eur.* **2001**, *2*, 91.
(43) Bader, R. F. *Atoms in Molecules: A Quantum Theory*; Oxford Science Publications, Clarendon Press: Oxford, 1990.
(44) Foresman, J. B.; Frisch, A. *Exploring Chemistry with Electronic Structure Methods*, 2nd ed.; Gaussian, Inc: Pittsburgh 1996.
(45) Scott, A. P.; Radom, L. *J. Phys. Chem.* **1996**, *100*, 16502.
(46) Rauhut, G.; Pulay, P. *J. Am. Chem. Soc.* **1995**, *117*, 4167.
(47) Baker, J.; Jarzecki, A. A.; Pulay, P. *J. Phys. Chem. A* **1998**, *102*, 1412.
(48) Tantirungrotechai, Y.; Phanasant, K.; Roddecha, S.; Surawatanawong, P.; Sutthikhum, V.; Limtrakul, J. *J. Mol. Struct. (THEOCHEM)* **2006**, *760*, 189.
(49) Åkesson, R.; Pettersson, L. G. M.; Sandström, M.; Wahlgred, U. *J. Am. Chem. Soc.* **1994**, *116*, 8691.
(50) Ducommun, Y.; Newman, K. E.; Merbach, A. E. *Inorg. Chem.* **1980**, *19*, 3696.
(51) Desai, A. G.; Dodgen, H. W.; Hunt, J. P. *J. Am. Chem. Soc.* **1970**, *92*, 798.
(52) Helm, L.; Merbach, A. E. *Chem. Rev.* **2005**, *105*, 1923.
(53) Gibbs, G. V.; Tamada, O.; Boisen, M. B.; Hill, F. C. *Am. Mineral.* **1999**, *84*, 435.
(54) Coppens, P. *Acta Crystallogr.* **1998**, *A54*, 779.
(55) Frenking, G.; Pidun, U. *J. Chem. Soc., Dalton Trans.* **1997**, *1653*.
(56) Erras-Hanauer, H.; Clark, T.; van Eldik, R. *Coord. Chem. Rev.* **2003**, *233*, 238–239.
(57) Fouqueau, A.; Mer, S.; Casida, M. E.; Daku, L. M. L.; Hauser, A.; Mineva, T.; Neese, F. *J. Chem. Phys.* **2004**, *120*, 9473.
(58) Partridge, H.; Bauschlicher, C. W. *J. Phys. Chem.* **1992**, *96*, 8827.
(59) Dudev, T.; Cowan, J. A.; Lim, C. *J. Am. Chem. Soc.* **1999**, *121*, 7665.
(60) Rustad, J. R.; Dixon, D. A.; Rosso, K. M.; Felmy, A. R. *J. Am. Chem. Soc.* **1999**, *121*, 3234.
(61) Hancock, R. D.; Bartolotti, L. J. *Inorg. Chem.* **2005**, *44*, 7175.
(62) Martell, A. E.; Smith, R. M.; Motekaites, R. J. *NIST Criticially Selected Stability Constants of Metal Complexes, V. 8.0*; NIST: Gaithersburg, 2004.
(63) Dimmock, P. W.; Warwick, P.; Robbins, R. A. *Analyst* **1995**, *120*, 2159.
(64) Gersten, G. I.; Foley, H. M. *Phys. Rev.* **1969**, *182*, 24.
(65) Boese, R.; Niederprum, N.; Blaser, D.; Manlitz, A.; Antipin, M. Y.; Mallinson, P. R. *J. Phys. Chem. B* **1997**, *101*, 5794.
(66) Computational Chemistry Comparison and Benchmark Database (CCCBDB); NIST Standard Reference Database 101, 2006.
(67) Clough, S. A.; Beers, Y.; Klein, G. P. *J. Chem. Phys.* **1973**, *59*, 2254.
(68) Eisenberg, D.; Kauzmann, W. *The Structure and Properties of Water*; Clarendon Press: Oxford 1969.

JP803961S